Front. Optoelectron. China 2010, 3(3): 217–227
DOI 10.1007/s12200-010-0110-0

REVIEW ARTICLE

Fully transparent flexible transistors built on metal oxide nanowires

Di CHEN[1], Jing XU[1,2], Guozhen SHEN (✉)[1]

1 Wuhan National Laboratory for Optoelectronics, College of Optoelectronic Science and Engineering, Huazhong University of Science and Technology, Wuhan 430074, China
2 School of Chemistry and Chemical Engineering, Huazhong University of Science and Technology, Wuhan 430074, China

© Higher Education Press and Springer-Verlag Berlin Heidelberg 2010

Abstract Transparent electronics has attracted great research efforts in recent years due to its potential to make significant impact in many area, such as next generation displays, ultraviolet (UV) detectors, solar cells, charge-coupled devices (CCDs), and so on. Central to the realization of transparent electronics is the development of high performance fully transparent thin-film transistors (TFTs). One-dimensional (1-D) nanostructures have been the focus of current researches due to their unique physical properties and potential applications in nanoscale electronics and optoelectronics. Among 1-D nanostructures, transparent metal oxide nanowires are one of the best candidates to make fully transparent TFTs. We provide in this paper the most recent development on the fabrication of fully transparent TFT using metal oxide nanowires as the device elements. First, the review article gives a general introduction about the development of transparent electronics using different kinds of materials as the devices elements, including organic semiconductors, metal oxide thin films, and metal oxide nanowires. Second, the growth of metal oxide nanowires using vapor phase methods governed by two different growth mechanisms: vapor-solid mechanism and vapor-liquid-solid mechanism, respectively, are described. Third, the fabrication of transparent and flexible TFTs using different metal oxides nanowires is comprehensively described. In conclusion, the challenges and prospects for the future are discussed.

Keywords thin-film transistor (TFT), field-effect transistor (FET), transparent electronics, nanowires, metal oxide

1 Introduction

Acting as one of the emerging technology for the next generation of optoelectronic devices, transparent electronics, also called invisible electronics, has attracted great interests in recent years due to its great potential to make significant impact in a wide variety of areas, such as ultraviolet (UV) detectors, solar cells, charge-coupled devices (CCDs), and especially next generation transparent displays [1–5]. Central to the realization of transparent electronics is the development of thin-film transistors (TFTs) with high mobility. The realization of entirely transparent displays needs not only transparent light-emitting devices but also a driving scheme based on transparent TFTs. When made on flexible plastic substrate, low-temperature fabrication process is essential since plastic substrate cannot work at high temperature [6,7].

TFTs fabricated by using organic semiconductors as the channel materials were widely investigated over the past years due to their materials variation, compatible to plastic substrate, good transparency, and good printable nature [8–16]. Organic TFTs (OTFTs) based on conjugated polymers, oligomers, or fused aromatics act as a viable alternative to traditional inorganic TFTs. The highest mobility obtained on OTFTs is pentacene-based OTFTs [8]. Though great efforts have been paid to improve the mobility of OTFTs, the mobilities of most of the reported OTFTs are still quite low even when compared with amorphous silicon TFTs. Another problem that should be considered for OTFTs is that organic semiconductors are sensitive to atmosphere, which prevents their wide applications in some special environments.

In the past few years, transparent TFTs made from metal oxide semiconductors have seen much significant progress. As-used metal oxides include zinc oxide (ZnO), tin dioxide (SnO_2), indium oxide (In_2O_3), indium-gallium oxide (IGO), and amorphous oxides, such as

Received April 19, 2010; accepted May 14, 2010

E-mail: gzshen@mail.hust.edu.cn

indium-gallium-zinc oxides (IGZO), cadmium-indium-antimony oxides (CIAO), etc. [17–24]. Metal oxide semiconductors are very attractive materials because they exhibit tunable conductance with high visual transparency. Transparent TFTs built on metal oxide thin films usually show much higher device mobilities when compared with amorphous Si-TFTs and OTFTs. Figure 1(a) is a photograph of ZnO-based transparent transistor. The coin under the device can be clearly seen through the device, indicating very good transparency. Figure 1(b) shows a magnified image of a bottom-gate transparent transistor. To fabricate the device, indium-tin oxide (ITO) was used as the gate electrode, and aluminum-titanium oxide (ATO) served as the gate dielectric. Nomura et al. fabricated transparent TFTs using single crystalline thin-film transparent oxide semiconductor and $InGaO_3(ZnO)_5$ as the electron channel. Though this is not the first report on transparent TFTs, the mobility Nomura et al. obtained is the highest one, which is around 80 $cm^2 \cdot V^{-1} \cdot s^{-1}$, compared with 0.3 to 2.5 $cm^2 \cdot V^{-1} \cdot s^{-1}$ for other ZnO-based transparent TFTs. Inspired by this work, researchers around the world paid great efforts to improve the performance of oxide thin-film-based transparent TFTs, especially the device mobilities, and there are still a lot of work to do to make full use of this kind of transparent TFTs.

Representing the smallest dimension structure that can efficiently transport electrical carriers, one-dimensional (1-D) nanostructures attracted great intention recently. They can be rationally synthesized in a single crystal form with controlled key parameters during growth, such as chemical composition, doping state, diameter, length, morphology, etc. The ability to produce 1-D nanostructures with controlled key parameters makes it possible to fabricate functional nanoscale devices [25–45]. For example, 1-D nanostructures have been assembled into nanoscale field-effect transistors (FETs), p-n diodes, UV detectors, light-emitting diode (LED), nanolasers, integrated nanowire devices, single nanowire solar cells, chemical sensors, biosensors, and nanogenerators. 1-D nanostructures, including carbon nanotubes and metal oxide nanowires, were considered as material candidates for transparent TFTs recently [46–51]. Using transfer printed aligned carbon nanotubes, we fabricated transparent TFTs on glass substrates and transparent flexible TFTs on PET substrates. Device mobility higher than 1300 $cm^2 \cdot V^{-1} \cdot s^{-1}$ was obtained. As-obtained transparent TFTs were also used to fabricate transparent inverter and to drive GaN-based LEDs. Metal oxide nanowires are another group of 1-D nanostructures that can be used to fabricate high-performance transparent flexible TFTs.

This paper reviews the state-of-the-art research activities in transparent flexible TFTs using metal oxide nanowires as the channel layers. First, the review article gives a general introduction about the development of transparent electronics using different kinds of materials as the devices elements, including organic semiconductors, metal oxide thin films, and metal oxide nanowires. Second, the growth of metal oxide nanowires using vapor phase methods governed by two different growth mechanisms: vapor-solid (VS) mechanism and vapor-liquid-solid (VLS) mechanism, respectively, are described. Third, the fabrication of transparent and flexible TFTs using different metal oxides is comprehensively described. In conclusion, the challenges and prospects for future development are discussed.

2 Synthesis of metal oxide nanowires

Vapor-phase methods are promising techniques to synthesize single crystalline metal oxide nanowires with excellent crystallinity and electric properties. They are usually governed by two different growth mechanisms: VS mechanism and VLS mechanism, respectively. For the VS process, the source was evaporated to generate the target vapors, which were transferred by the carrier gases to the low temperature region of the reaction system. The target vapors then directly deposited on the substrate located in the low temperature region to form the final 1-D nanostructures. Direct difference between these two

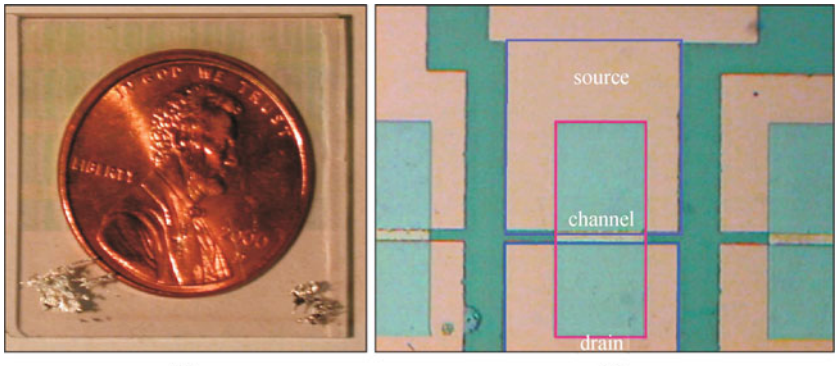


Fig. 1 ZnO-based transparent transistors. (a) Photograph of transparent device (a coin can be easily seen through the device); (b) enhanced-contrast, magnified image of a bottom-gate transparent transistor (Reprinted with permission from Ref. [1])

mechanisms is whether metal catalysts are used to promote the growth into 1-D nanostructure or not. Almost all metal oxides nanowires are reported until now. For example, 1-D nanostructures of tin oxide (SnO_2), indium oxide (In_2O_3), and zinc oxide (ZnO) can be synthesized using both VS process and VLS process. In this section, we briefly introduce the synthesis of metal oxide nanowires (SnO_2, In_2O_3, and ZnO) via the vapor-phase methods.

Figure 2 shows the scanning electron microscope (SEM) and transmission electron microscope (TEM) image of VS-grown SnO_2 nanobelts [52]. The ribbon-like morphology can be clearly seen in Figs. 2(b) and 2(c). Ripple-type contrast was seen in the TEM images, indicating the presence of strain. From these images, we can also see that the width and thickness of each SnO_2 nanoribbon are rather uniform, and the variation of the width is 30–200 nm. Studies found that these nanoribbons are single crystals with the growth direction close to the (101) plane. For the synthesis of SnO_2 nanobelts here, no catalyst was used, and a VS mechanism was thus used to explain the growth mechanism. During the synthesis, SnO_2 powders were evaporated at high temperature in a quartz tube furnace to generate SnO_2 vapors, which were then transferred by the carrier gases to the low temperature. They were then deposited on the substrate and grew into the final nanobelts. Similar methods were also used to synthesize SnO_2 nanowires, ZnO nanowires, ZnO nanobelts, ZnO nanotubes, In_2O_3 nanowires, and In_2O_3 nanobelts, etc. [53–55].

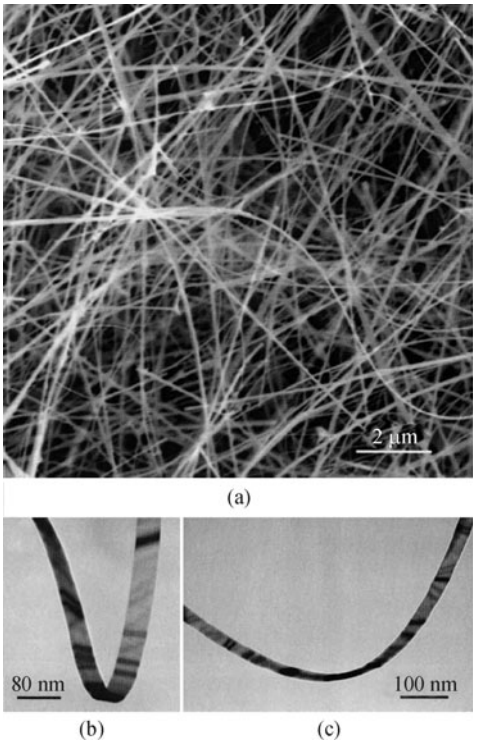


Fig. 2 (a) SEM image and (b), (c) TEM images of VS-grown SnO_2 nanobelts (Reprinted with permission from Ref. [52])

The diameter, length, and morphology of the produced metal oxide nanowires can be easily controlled during the VS process by control of experimental parameters, like temperature, source material, flowing gas, etc. Figure 3 demonstrates a series of SEM images of VS-grown ZnO nanowires with different tip structures [56,57]. All of these ZnO nanowires were produced by thermal evaporating zinc powders covered on indium film in a round-to-round metal vapor deposition route at 550°C. The only difference is the different amount of indium film. Tiny difference in source material resulted in great difference in tip structures of ZnO nanowires as revealed in these images.

Figure 4(a) shows the SEM image of In_2O_3 nanowires, which were synthesized via a laser ablation process. During this process, an InAs target was used as the source, and gold nanoparticle coated Si was used as the substrate to collect the final product. The reaction was performed at 700°C, and pure Ar gas was used as the carrier gas. Large quantity of In_2O_3 nanowires were found deposited on the substrate, as illustrated in Fig. 4(a). Figure 4(b) is a TEM image of the deposited In_2O_3 nanowires. Small particles were found attached to the tips of the nanowires, indicating the typical VLS mechanism. As-synthesized nanowires have diameters of 20–40 nm and lengths up to several tens of micrometers. A high-resolution TEM (HRTEM) image of the synthesized In_2O_3 nanowire is shown in Fig. 4(c). The clearly resolved lattice fringe is 0.506 nm, corresponding to the (200) plane of cubic In_2O_3 crystal structure. The results indicate that the In_2O_3 nanowires grown using the laser ablation process are single crystals with high crystalline quality. The laser ablation process was also used to synthesize SnO_2 nanowires under similar conditions [58,59].

3 Transparent flexible TFTs with metal oxide nanowires

The ability to produce a wide range of metal oxide nanowires with controlled composition, size, shapes, and properties opens up many exciting opportunities ranging from fundamental studies of the dimension-related physical properties to potential applications in nanoscale electronics, optoelectronics, sensors, and many others. In this section, we will introduce the interesting application of metal oxide nanowires to make fully transparent flexible transistors.

Lu et al. reported the studies of transparent TFT devices based on lightly Ta-doped SnO_2 nanowires [60]. SnO_2 nanowires were chosen as the channel material due to the low growth cost, high optical transmittance, and good electronic properties. Lightly, Ta-doped SnO_2 nanowires were synthesized at 900°C by a catalyst-mediated VLS process, in which the Ta and Sn source materials were provided by a chemical vapor deposition method. The synthesized Ta-doped SnO_2 nanowires are perfect single

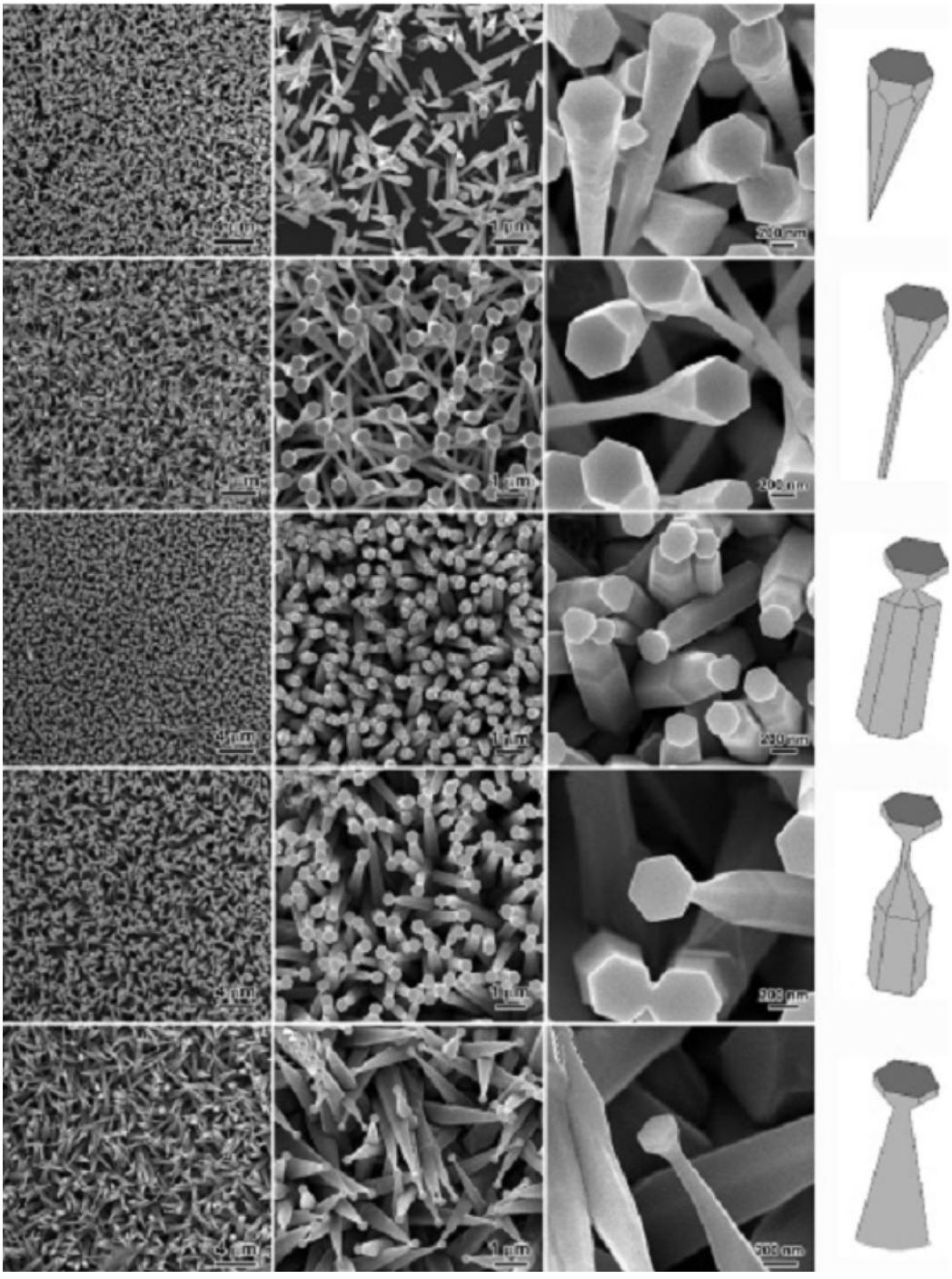


Fig. 3 SEM images of VS-grown ZnO nanowires with controlled tip structures (Reprinted with permission from Ref. [56])

crystals with no visible dislocations and amorphous surface overcoating and growing along the (101) plane.

After synthesis, the Ta-doped SnO_2 nanowires were transferred onto a Pyrex glass substrate using a physical transfer method. Figure 5(a) shows a dark-field optical microscope image of the nanowire film obtained through the physical transfer method. Most of the transferred nanowires are parallel to each other as indicated in the image. After transferring, conventional sputter, photolithography, and liftoff processes were used to pattern the device structure, which was demonstrated in Fig. 5(b). During device fabrication process, the highest temperature used was limited to 250°C, making it compatible with certain plastic substrates for applications of transparent flexible electronics. The device after fabrication was depicted in Fig. 5(c). The device exhibits excellent

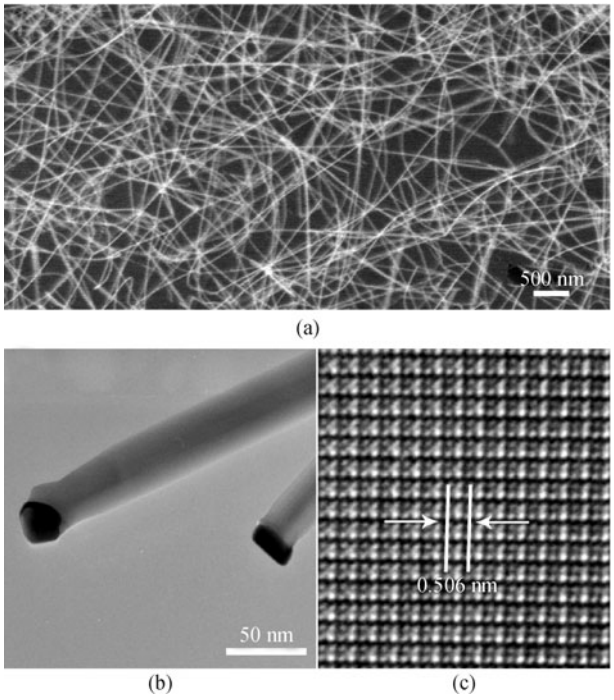


Fig. 4 (a) SEM image, (b) TEM image, and (c) HRTEM image of laser ablation synthesized In_2O_3 nanowires

transparency, and the back image can be clearly seen through the device. An optical transmittance spectrum of the device on glass was shown in Fig. 5(d), showing a transmittance of ~70%, including the Pyrex glass substrate.

Figure 6 is the electrical characterizations obtained on a top-gated nanowire TFT device with a *W*/*L* ratio of 12.6. A dark-field microscope image of the device is shown in Fig. 6(a) inset. From these curves, one can see that the device displays very good n-type transistor behavior with clear linear and saturation regions. A large on current of 71 μA and an on/off ratio of ~10^3 can be obtained within a small V_{dd} bias window of 2.5 V. The nanowire-based TFT device shows better performance within a smaller V_{dd} bias window compared with amorphous or polycrystalline transparent TFT devices fabricated near room temperature. After calculation, the transparent TFT device shows device mobility over 100 $cm^2 \cdot V^{-1} \cdot s^{-1}$.

Using In_2O_3 nanowires as the channel material, researchers in Purdue University, Northwestern University, and University of Southern California fabricated fully transparent and flexible nanowire transistors on plastic substrate [61]. The In_2O_3 nanowires were prepared from the laser ablation assisted VLS process using InAs as the target. Figure 7(a) is the cross-sectional view of the fully transparent and flexible nanowire device structure, which is composed of a transparent plastic substrate, transparent patterned ITO gate electrode, transparent atomic layer deposition (ALD) deposited Al_2O_3 gate insulator, In_2O_3 nanowires as the active channel, and transparent ITO as the source/drain electrodes. As-fabricated nanowire device shows excellent transmittance and flexibility, as revealed in Figs. 7(b) and 7(c). A transmittance of ~81% was obtained, as shown in Fig. 7(c). Figure 7(d) shows the $I_{ds} - V_{gs}$ curves of a representative nanowire device as well as the field effect mobilities of typical devices. An on/off ratio of ~10^5 and mobilities ranging from 120 to 167 $cm^2 \cdot V^{-1} \cdot s^{-1}$ were

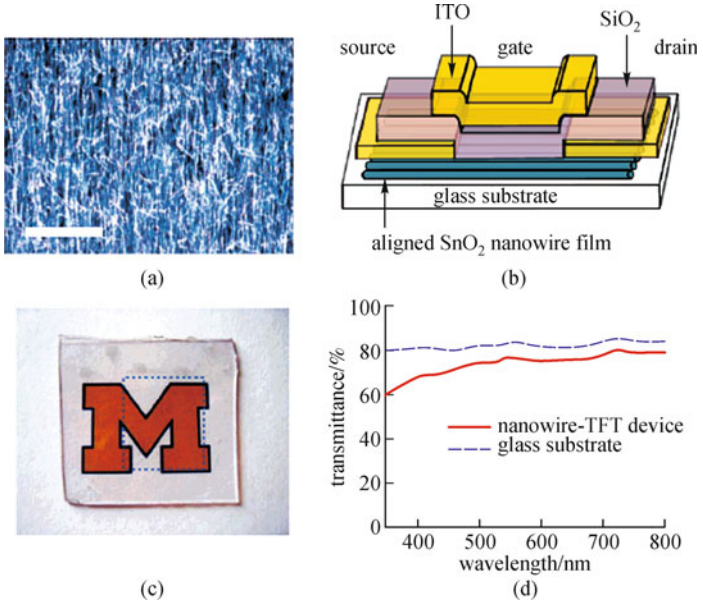


Fig. 5 (a) Dark-field optical microscope image of an SnO_2 nanowire film obtained through physical transfer method (scale bar: 20 μm); (b) schematic of transparent SnO_2 nanowire-based TFT device; (c) digital photograph of a 200-device array of nanowire-TFTs fabricated on Pyrex glass; (d) optical transmittance spectrum of nanowire-TFT device array on glass substrate (solid line) and glass substrate alone (dashed line) (Reprinted with permission from Ref. [60])

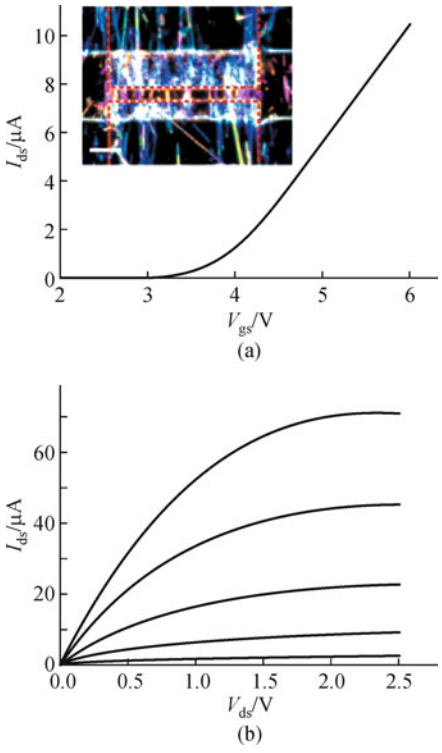


Fig. 6 (a) I_{ds}–V_{gs} curve at V_{ds}= 0.1 V; (b) family of I_{ds}–V_{gs} curves for the same device with V_{gs} = 6.0 to 3.5 V in –0.5 V steps (Reprinted with permission from Ref. [60])

obtained for the In_2O_3 nanowire devices. Similarly, they also fabricated nanowire transistor devices using ZnO nanowires as the active channels.

Possible applications of the transparent and flexible nanowire transistors include pixel drivers for active matrix organic light-emitting diode (AMOLED) displays since nanowire transistors offer the performance required for AMOLED circuitry along with desired transparency and processing characteristics. Ju et al. reported the first transparent AMOLED display elements in which the switching and driving circuits are comprised exclusively of nanowire transistor electronics fabricated at room temperature [62]. For transparent and flexible displays, the realization of transparent transistor and circuit integration strategies are required, and for each active matrix (AM) display pixel, it must contain at least one switching transistor, one driver transistor, and a storage capacitor, with appropriate scan and data lines to allow selective pixel addressing. Figure 8(a) is the optical image of the fully transparent nanowire AMOLED substrate. The background image is clearly visible through the display region. Optical images of the nanowire AMOLED array in the off state and on state are shown in Fig. 8(b). Optical transmittance of ~72% and ~35% are obtained for the display before and after OLED deposition, respectively, as indicated in Fig. 8(c). The transmittance of the display should be improved if better transparent materials are used. The results indicate that nanowire transistor device strategies can be optimized for the requirement of applications, such as displays, head-mounted displays, transparent screen monitors, etc.

Besides, radio-frequency characterization of fully transparent nanowire TFTs was also carried out. For example, Lu et al. fabricated fully transparent nanowire TFTs on glass substrate by using VLS-grown SnO_2 nanowires as the transistor active channel materials [63]. For the device built on aligned SnO_2 nanowire arrays, a current-gain cutoff frequency of 109 MHz and a power-gain cutoff frequency of 286 MHz were obtained.

For the vapor phase synthesized metal oxide nanowires, the electronic properties may be tuned by introducing proper dopants, thus making it possible to make high-performance fully transparent, flexible transistors with tunable device mobility, or on/off ratios. Lee et al. fabricated fully transparent and flexible transistors using zinc-doped indium oxide nanowires as the active channel materials [64]. The Zn-In_2O_3 nanowires with diameters of 80–100 nm and lengths of 20–50 μm were synthesized via a VS process. The doping effect was determined by measuring the resistivity of the nanowires with and without zinc dopant, respectively. The resistivity of the doped nanowires is $2.15\times10^{-2}\,\Omega\cdot$cm, which is one order of magnitude lower than undoped nanowires. Fully transparent and flexible nanowire transistors were fabricated by combining the Zn-In_2O_3 nanowires channel, a SiN_x high-κ gate dielectric, and transparent ITO electrodes on a PET substrate. As-fabricated devices showed high carrier mobilities of $631\,cm^2\cdot V^{-1}\cdot s^{-1}$, large on/off ratio of 1×10^6, and a high on-state current of 1×10^{-5} A. No obvious performance degradation was observed after bending the device, indicating stable performance.

Using a laser ablation chemical vapor deposition (CVD) method, we synthesized single-crystalline As-doped In_2O_3 nanowires on a large scale [65]. As-synthesized nanowires grew along the (100) direction. After synthesis, the nanowires were dispersed into isopropyl alcohol (IPA) and then dispersed onto an ITO substrate with 50 nm Al_2O_3 dielectric until desired nanowire density was obtained. Figure 9(a) is a schematic of an As-doped In_2O_3 nanowire transparent TFT on glass substrate. The device shows very good optical transparency, which can be seen in Fig. 9(b), where the background photography visible through the transistor regions. The electric transport behaviors of the fabricated devices were also studied, and the results were listed in Figs. 9(c) and 9(d). From these results, we can see that the device exhibits typical enhancement-mode n-type semiconductor transistor behavior with high on/off ratio of 5.7×10^6 and high device mobility ranging from 1080 to $1490\,cm^2\cdot V^{-1}\cdot s^{-1}$.

The above As-In_2O_3 nanowire transparent TFTs with high device mobility may be employed as switching and driving transistors in an AMOLED display circuitry. Figure 10(a) is an equivalent circuit diagram of

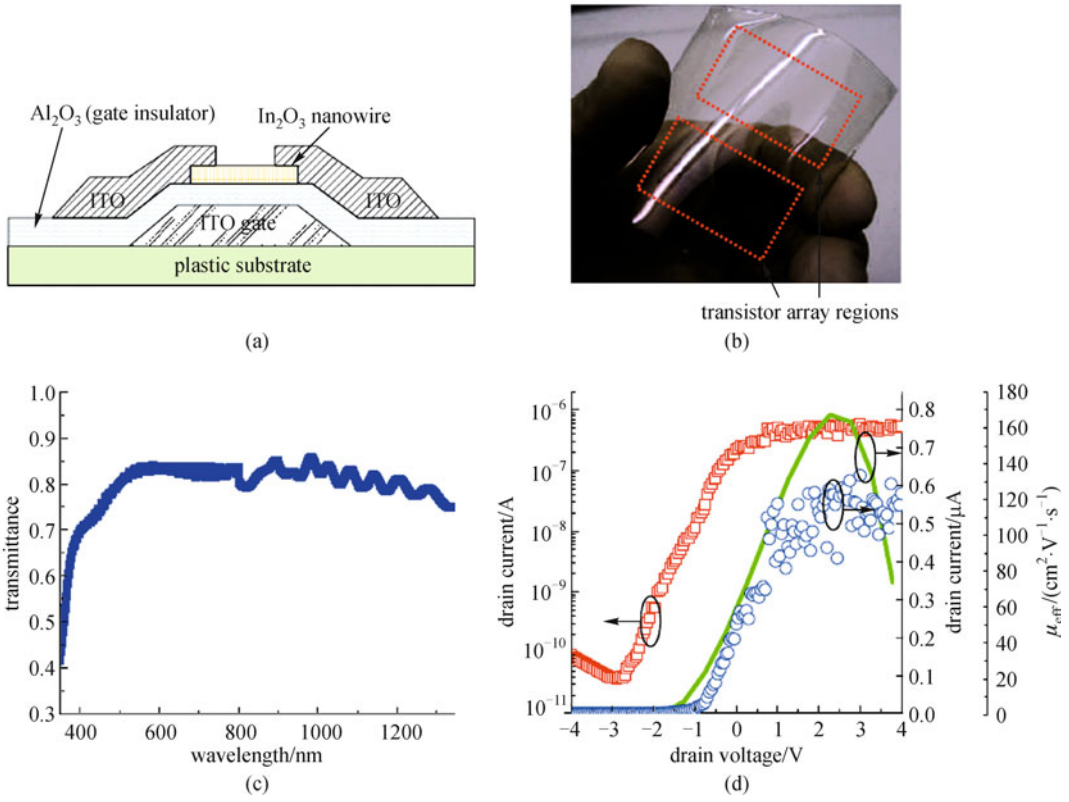


Fig. 7 (a) Cross-sectional view of fully transparent and flexible nanowire transistor device; (b) image of In_2O_3 nanowire transistors on plastic substrate, showing the optical clarity and mechanical flexibility; (c) optical transmission spectrum of the device; (d) I_{ds}–V_{gs} characteristic of In_2O_3 nanowire transistors at V_d = 0.5 V, where blue, red, and green data points correspond to linear-scale I_{ds}–V_{gs}, log-scale I_{ds}–V_{gs}, and μ_{eff}, respectively. Arrows indicate appropriate axis (Reprinted with permission from Ref. [61])

seven-segment AMOLED display circuitry. Each OLED pixel consists of one switching transistor, one driving transistor, and one storage capacitor. Figure 10(b) shows the optical image of the AMOLED display substrate before OLED deposition. It still shows good transparency, and the background image is still visible through the display region. To demonstrate the application as AMOLED display, we showed optical images of the seven-segment pixels with different numerical digits at different data line voltage with different scan line voltages, as shown in Fig. 10(c). The digital number "1", "3", and "6" can be easily seen from the images.

We show above that metal oxide nanowires may be used to fabricate high-performance transparent flexible transistors. However, to realize fully transparent and/or flexible nanoscale devices, transparent, and/or flexible energy conversion and storage units, transparent contact layers should also be considered. Previously, we fabricated transparent and flexible supercapacitor based on In_2O_3 nanowire/carbon nanotube heterogeneous films [66]. The power density of which can reach 7.48 kW/kg, and a good retention of capacity was obtained. For the transparent contact layer material, O'Dwyer et al. synthesized transparent indium tin oxide nanowires using a controllable molecular beam epitaxy (MBE) system [67].

4 Conclusion and remarks

In conclusion, a comprehensive review of the state-of-the-art research activities of interesting fully transparent flexible transistors, in which metal oxide nanowires are used as the acting channel materials, are provided here. The synthesis of metal oxides by using vapor phase methods and the fabrication of fully transparent and/or flexible transistors by using metal oxide nanowires as the active channel materials are reviewed in the paper in order to give the readers a clear map of this interesting research topic. Metal oxide nanowires act as one of the best candidates for the fabrication of high-performance fully transparent flexible transistors. In addition, we believe that the fascinating achievements in this topic should inspire more and more research efforts to address the remaining challenges.

This interesting topic was only developed for the last several years, and we believe that there is still plenty of

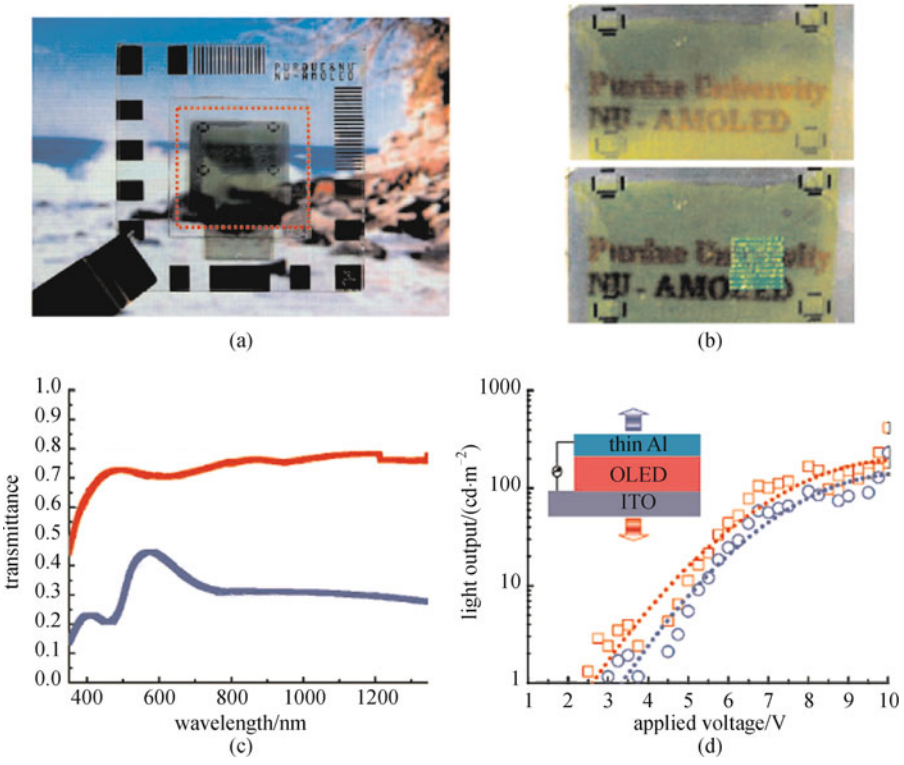


Fig. 8 (a) Optical image of fully transparent nanowire AMOLED substrate; (b) optical images of a region of substrate containing a 2 mm×2 mm array; (c) optical transmission spectrum of nanowire AMOLED display substrate before and after OLED deposition; (d) measured luminance versus supply voltage curve for AMOLED array with all scan and data lines enabled (Reprinted with permission from Ref. [62])

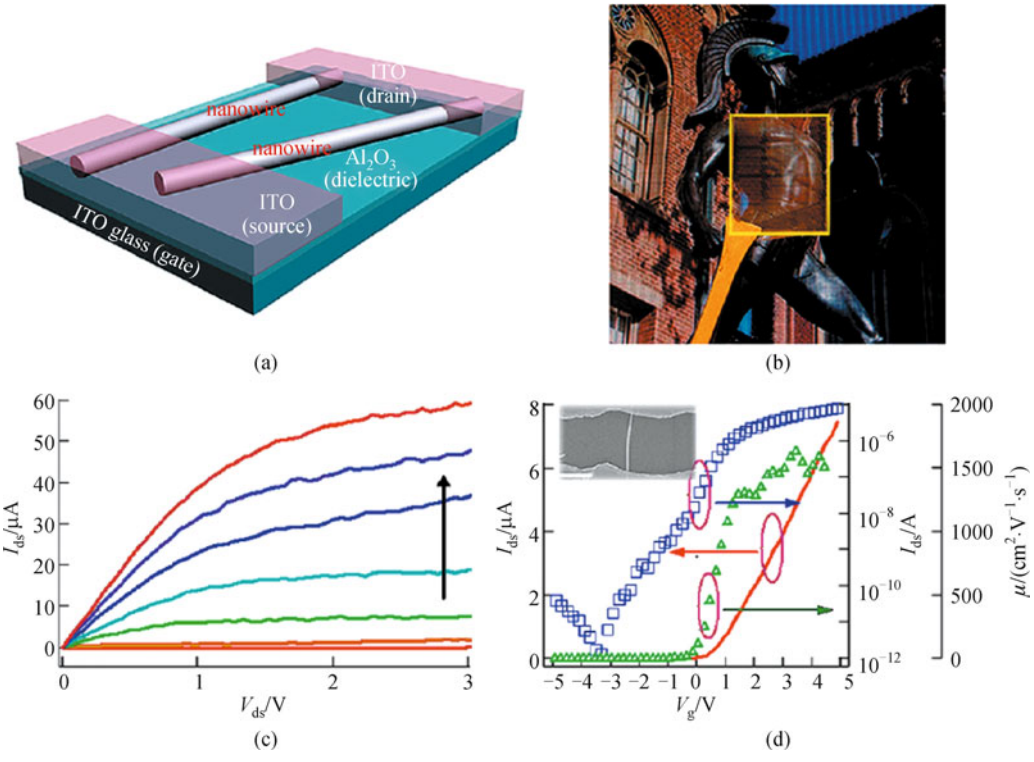


Fig. 9 (a) Schematic of As-doped In_2O_3 nanowire transparent TFTs; (b) optical image of fully transparent TFTs built on As-doped In_2O_3 nanowires; (c) family of I_{ds}–V_{ds} curves of a single TFT; (d) current versus gate voltage plot in linear regime (Reprinted with permission from Ref. [65])

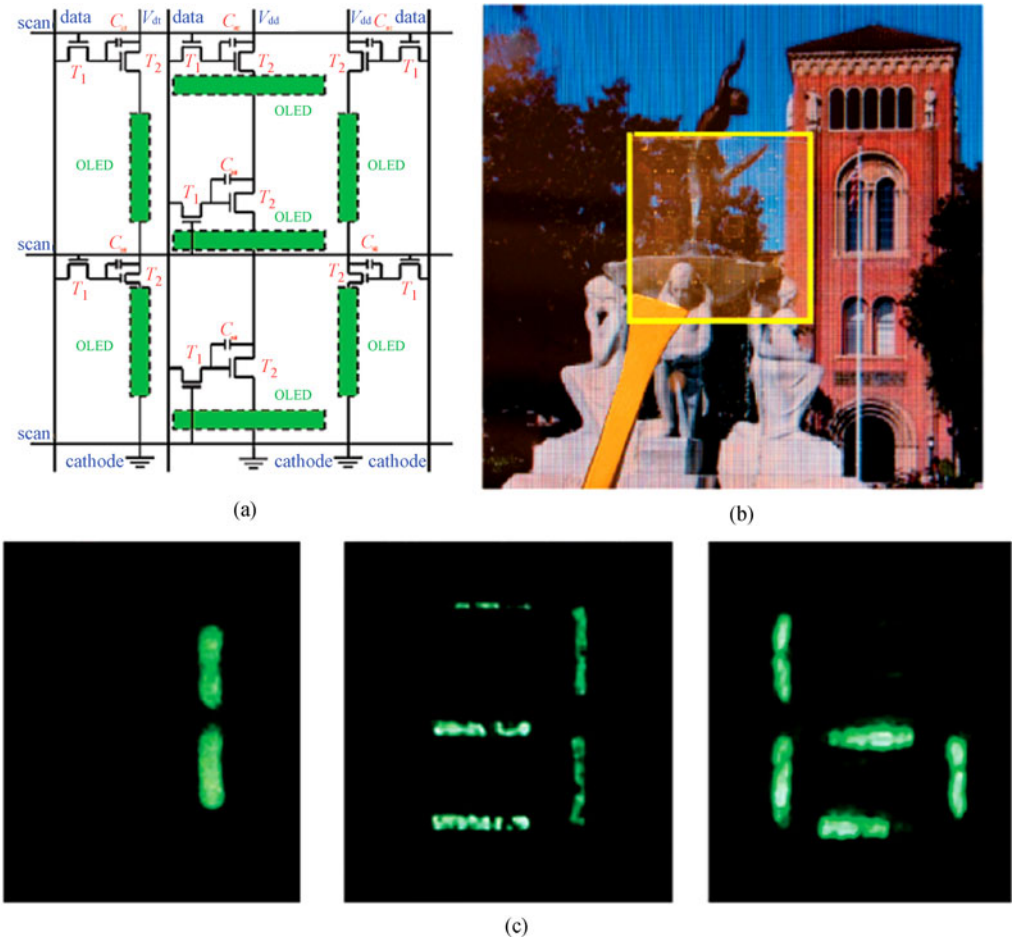


Fig. 10 Application of As-doped In_2O_3 nanowire transparent TFTs circuitry to drive seven-segment AMOLED display. (a) Equivalent circuit diagram of seven-segment AMOLED display circuitry; (b) optical image of AMOLED display substrate before OLED deposition; (c) optical images of seven-segment pixels with different numerical digits (number "1", "3", and "6" can be easily seen) (Reprinted with permission from Ref. [65])

room for researchers to explore. Synthesizing metal oxide nanowires with excellent electrical properties is one of the most difficult challenges. Using vapor phase methods, people are able to control the diameters, lengths, and shapes, now. However, the complicated environments within the vapor phase system make it difficult to control the electrical properties of the nanowires synthesized, which then makes it difficult to fabricate high-performance fully transparent flexible transistors.

Second, techniques focusing on transferring metal oxide nanowires to the device substrate, for example, glass, PET, etc., are required to decrease the lose of metal oxide nanowires.

Third, the device structures and fabrication procedures should be improved to optimize the performance of the final devices. For example, the performance of the devices is greatly influenced by the thickness and material of dielectric layers and source/drain electrodes.

Finally, to realize fully transparent and/or flexible nanoscale devices, other items besides transparent transistors should also be considered and should be explored, for example, the transparent dielectric layers, the transparent electrodes, and even the transparent energy conversion and storage units.

Acknowledgements This work was supported by the High-level Talent Recruitment Foundation of Huazhong University of Science and Technology, the Natural Science Foundation of Hubei Province (No. 2009CDB326), the Research Fund for the Doctoral Program of Higher Education (No. 20090142120059), and the Basic Scientific Research Funds for Central Colleges (No. Q2009043). The authors are indebted for the kind permissions from the corresponding publishers, or authors to reproduce their published materials, especially figures, used in this review.

References

1. Wager J F. Transparent electronics. Science, 2003, 300(5623): 1245–1246
2. Wagner J F, Keszler D A, Presley R E. Transparent Electronics. New York: Springer, 2008

3. Kawazoe H, Yasukawa M, Hyodo H, Kurita M, Yanagi H, Hosono H. P-type electrical conduction in transparent thin films of $CuAlO_2$. Nature, 1997, 389(6654): 939–942
4. Nomura K, Ohta H, Takagi A, Kamiya T, Hirano M, Hosono H. Room-temperature fabrication of transparent flexible thin-film transistors using amorphous oxide semiconductors. Nature, 2004, 432(7016): 488–492
5. Chiang H Q, Wager J F, Hoffman R L, Jeong J, Keszler D A. High mobility transparent thin-film transistors with amorphous zinc tin oxide channel layers. Applied Physics Letters, 2005, 86(1): 013503
6. Görrn P, Sander M, Meyer J, Kroger M, Becker E, Johannes H H, Kowalsky W, Riedl T. Towards see-through displays: fully transparent thin-film transistors driving transparent organic light-emitting diodes. Advanced Materials, 2006, 18(6): 738–741
7. Wang L, Yoon M H, Lu G, Yang Y, Facchetti A, Marks T J. High-performance transparent inorganic-organic hybrid thin-film n-type transistors. Nature Materials, 2006, 5(11): 893–900
8. Lin Y Y, Gundlach D J, Nelson S, Jackson T N. Stacked pentacene layer orgainc thin-film transistors with improved characteristics. IEEE Electron Device Letters, 1997, 18(12): 606–608
9. Bao Z, Lovinger A J, Dodabalapur A. Organic field-effect transistors with high mobility based on copper phthalocyanine. Applied Physics Letters, 1996, 69(20): 3066–3068
10. Katz H E. Organic molecular solids as thin film transistor semiconductors. Journal of Materials Chemistry, 1997, 7(3): 369–376
11. Horowitz G. Organic field-effect transistors. Advanced Materials, 1998, 10(5): 365–377
12. Garnier F. Thin film transistors based on organic conjugated semiconductors. Chemical Physics, 1998, 227(1–2): 253–262
13. Choi Y W, Kim I D, Tuller H L, Akinwande A I. Low-voltage organic transistors and depletion-load inverters with high-*K* pyrochlore BZN gate dielectric on polymer substrate. IEEE Transactions on Electron Devices, 2005, 52(12): 2819–2824
14. Tsumura A, Koezuka H, Ando T. Macromolecular electronic devices: field-effect transistor with a polythiophene thin film. Applied Physics Letters, 1986, 49(18): 1210–1212
15. Klauk H, Halik M, Zschieschang U, Eder F, Rohde D, Schmid G, Dehm C. Flexible organic complementary circuits. IEEE Transactions on Electron Devices, 2005, 52(4): 618–622
16. Na J H, Kitamura M, Lee D, Arakawa Y. High performance flexible pentacene thin-film transistors fabricated on titanium silicon oxide gate dielectrics. Applied Physics Letters, 2007, 90(16): 163514
17. Fortunato E M C, Barquinha P M C, Pimentel A C M B G, Gonçalves A M F, Marques A J S, Pereira L M N, Martins R F P. Fully transparent ZnO thin-film transistor produced at room temperature. Advanced Materials, 2005, 17(5): 590–594
18. Nomura K, Ohta H, Ueda K, Kamiya T, Hirano M, Hosono H. Thin-film transistor fabricated in single-crystalline transparent oxide semiconductor. Science, 2003, 300(5623): 1269–1272
19. Hosono H. Transparent amorphous oxide semiconductors for high performance TFT. SID Symposium Digest of Technical Papers, 2007, 38(1): 1830–1833
20. Presley R E, Munsee C L, Park C, Hong D, Wager J F, Keszler D A. Tin oxide transparent thin-film transistors. Journal of Physics D, 2004, 37(20): 2810–2813
21. Görrn P, Holzer P, Riedl T, Kowalsky W, Wang J, Weimann T, Hinze P, Kipp S. Stability of transparent zinc tin oxide transistors under bias stress. Applied Physics Letters, 2007, 90(6): 063502
22. Narushima S, Orita M, Hirano M, Hosono H. Electronic structure and transport properties in the transparent amorphous oxide semiconductor $2CdO \cdot GeO_2$. Physical Review B: Condensed Matter and Materials Physics, 2002, 66(3): 035203
23. Grover M S, Hersh P A, Chiang H Q, Kettenring E S, Wager J F, Keszler D A. Thin-film transistors with transparent amorphous zinc indium tin oxide channel layer. Journal of Physics D, 2007, 40(5): 1335–1338
24. Kumomi H, Nomura K, Kamiya T, Hosono H. Amorphous oxide channel TFTs. Thin Solid Films, 2008, 516(7): 1516–1522
25. Shen G Z, Chen P C, Ryu K, Zhou C. Devices and chemical sensing applications of metal oxide nanowires. Journal of Materials Chemistry, 2009, 19(7): 828–839
26. Curreli M, Li C, Sun Y, Lei B, Gundersen M A, Thompson M E, Zhou C. Selective functionalization of In_2O_3 nanowire mat devices for biosensing applications. Journal of the American Chemical Society, 2005, 127(19): 6922–6923
27. Tian B, Zheng X, Kempa T J, Fang Y, Yu N, Yu G, Huang J, Lieber C M. Coaxial silicon nanowires as solar cells and nanoelectronic power sources. Nature, 2007, 449(7164): 885–889
28. Qian F, Li Y, Gradecak S, Park H G, Dong Y, Ding Y, Wang Z L, Lieber C M. Multi-quantum-well nanowire heterostructures for wavelength-controlled lasers. Nature Materials, 2008, 7(9): 701–706
29. Law M, Greene L E, Johnson J C, Saykally R, Yang P. Nanowire dye-sensitized solar cells. Nature Materials, 2005, 4(6): 455–459
30. Wang Z L. Nanowires and Nanobelts: Materials, Properties and Devices. Boston: Kluwer Academic Publishers, 2003
31. Li Y, Qian F, Xiang J, Lieber C M. Nanowire electronic and optoelectronic devices. Materials Today, 2006, 9(10): 18–27
32. Meindl J D, Chen Q, Davis J A. Limits on silicon nanoelectronics for terascale integration. Science, 2001, 293(5537): 2044–2049
33. Shen G Z, Chen D, Chen P C, Zhou C. Vapor-solid growth of one-dimensional layer-structured gallium sulfide nanostructures. ACS Nano, 2009, 3(5): 1115–1120
34. Chen P C, Shen G Z, Zhou C. Chemical sensors and electronic noses based on 1-D metal oxide nanostructures. IEEE Transactions on Nanotechnology, 2008, 7(6): 668–682
35. Zhang J, Chen P C, Shen G Z, He J B, Kumbhar A, Zhou C, Fang J. P-type field-effect transistors of single-crystal zinc telluride nanobelts. Angewandte Chemie International Edition, 2008, 47 (49): 9469–9471
36. Shen G Z, Chen D. Self-coiling of $Ag_2V_4O_{11}$ nanobelts into perfect nanorings and microloops. Journal of the American Chemical Society, 2006, 128(36): 11762–11763
37. Cui Y, Wei Q, Park H, Lieber C M. Nanowire nanosensors for highly sensitive and selective detection of biological and chemical species. Science, 2001, 293(5533): 1289–1292
38. Huang Y, Duan X, Cui Y, Lauhon L J, Kim K H, Lieber C M. Logic gates and computation from assembled nanowire building blocks. Science, 2001, 294(5545): 1313–1317
39. Shen G Z, Bando Y, Hu J Q, Golberg D. High-symmetry ZnS hepta- and tetrapods composed of assembled ZnS nanowire arrays. Applied

Physics Letters, 2007, 90(12): 123101
40. Law M, Kind H, Messer B, Kim F, Yang P. Photochemical sensing of NO_2 with SnO_2 nanoribbon nanosensors at room temperature. Angewandte Chemie International Edition, 2002, 41(13): 2405–2408
41. Kolmakov A, Moskovits M. Chemical sensing and catalysis by one-dimensional nanostructures. Annual Review of Materials Research, 2004, 34: 151–180
42. Shen G Z, Bando Y, Ye C H, Yuan X L, Sekiguchi T, Golberg D. Single-crystal nanotubes of II_3-V_2 semiconductors. Angewandte Chemie International Edition, 2006, 45(45): 7568–7572
43. Duan X, Huang Y, Agarwal R, Lieber C M. Single-nanowire electrically driven lasers. Nature, 2003, 421(6920): 241–245
44. Zhong Z, Qian F, Wang D, Lieber C M. Synthesis of p-type gallium nitride nanowires for electronic and photonic nanodevices. Nano Letters, 2003, 3(3): 343–346
45. Zhong Z, Wang D, Cui Y, Bockrath M W, Lieber C M. Nanowire crossbar arrays as address decoders for integrated nanosystems. Science, 2003, 302(5649): 1377–1379
46. Cao Q, Hur S H, Zhu Z T, Sun Y, Wang C J, Meitl M A, Shim M, Rogers J A. Highly bendable, transparent thin-film transistors that use carbon-nanotube-based conductors and semiconductors with elastomeric dielectrics. Advanced Materials, 2006, 18(3): 304–309
47. Ishikawa F N, Chang H K, Ryu K, Chen P C, Badmaev A, Gomez De Arco L, Shen G Z, Zhou C W. Transparent electronics based on transfer printed aligned carbon nanotubes on rigid and flexible substrates. ACS Nano, 2009, 3(1): 73–79
48. Eda G, Fanchini G, Chhowalla M. Large-area ultrathin films of reduced graphene oxide as a transparent and flexible electronic material. Nature Nanotechnology, 2008, 3(5): 270–274
49. Artukovic E, Kaempgen M, Hecht D S, Roth S, Grüner G. Transparent and flexible carbon nanotube transistors. Nano Letters, 2005, 5(4): 757–760
50. Tseng S H, Tai N H. Fabrication of a transparent and flexible thin film transistor based on single-walled carbon nanotubes using the direct transfer method. Applied Physics Letters, 2009, 95(20): 204104
51. Bae E J, Min Y S, Kim U J, Park W J. Thin film transistors of single-walled carbon nanotubes grown directly on glass substrates. Nanotechnology, 2007, 18(49): 495203
52. Dai Z R, Pan Z W, Wang Z L. Ultra-long single crystalline nanoribbons of tin oxide. Solid State Communications, 2001, 118 (7): 351–354
53. Shen G Z, Bando Y, Lee C J. Growth of self-organized hierarchical ZnO nanoarchitectures by a simple thermal evaporation process. Journal of Physical Chemistry B, 2005, 109(21): 10779–10785
54. Shen G Z, Bando Y, Lee C J. Synthesis and evolution of novel hollow ZnO urchins by a simple thermal evaporation process. Journal of Physical Chemistry B, 2005, 109(21): 10578–10583
55. Shen G Z, Cho J H, Lee C J. Morphology-controlled synthesis, growth mechanism and optical properties of ZnO nanonails. Chemical Physics Letters, 2005, 401(4–6): 414–419
56. Shen G Z, Bando Y, Chen D, Liu B, Zhi C, Golberg D. Morphology-controlled synthesis of ZnO nanostructures by a simple round-to-round metal vapor deposition route. Journal of Physical Chemistry B, 2006, 110(9): 3973–3978
57. Shen G Z, Bando Y, Liu B, Golberg D, Lee C J. Characterization and field-emission properties of vertically-aligned ZnO nanonails and nanopencils fabricated by a modified thermal evaporation process. Advanced Functional Materials, 2006, 16(3): 410–416
58. Liu Z, Zhang D, Han S, Li C, Tang T, Jin W, Liu X, Lei B, Zhou C. Laser ablation synthesis and electronic transport studies of tin oxide nanowires. Advanced Materials, 2003, 15(20): 1754–1757
59. Li C, Zhang D, Han S, Liu X, Tang T, Zhou C. Diameter-controlled growth of single-crystalline In_2O_3 nanowires and their electronic properties. Advanced Materials, 2003, 15(2): 143–146
60. Dattoli E N, Wan Q, Guo W, Chen Y, Pan X, Lu W. Fully transparent thin-film transistor devices based on SnO_2 nanowires. Nano Letters, 2007, 7(8): 2463–2469
61. Ju S, Facchetti A, Xuan Y, Liu J, Ishikawa F, Ye P, Zhou C W, Marks T J, Janes D B. Fabrication of fully transparent nanowire transistors for transparent and flexible electronics. Nature Nanotechnology, 2007, 2(6): 378–384
62. Ju S, Li J, Liu J, Chen P C, Ha Y G, Ishikawa F N, Chang H K, Zhou C, Facchetti A, Janes D B, Marks T J. Transparent active matrix organic light-emitting diode displays driven by nanowire transistor circuitry. Nano Letters, 2008, 8(4): 997–1004
63. Dattoli E N, Kim K H, Fung W Y, Choi S Y, Lu W. Radio-frequency operation of transparent nanowire thin-film transistors. IEEE Electron Device Letters, 2009, 30(7): 730–732
64. Zhang W F, He Z B, Yuan G D, Jie J S, Luo L B, Zhang X J, Chen Z H, Lee C S, Zhang W J, Lee S T. High-performance, fully transparent, and flexible zinc-doped indium oxide nanowire transistors. Applied Physics Letters, 2009, 94(12): 123103
65. Chen P C, Shen G Z, Chen H, Ha Y G, Wu C, Sukcharoenchoke S, Fu Y, Liu J, Facchetti A, Marks T J, Thompson M E, Zhou C. High-performance single-crystalline arsenic-doped indium oxide nanowires for transparent thin-film transistors and active matrix organic light-emitting diode displays. ACS Nano, 2009, 3(11): 3383–3390
66. Chen P C, Shen G Z, Sukcharoenchoke S, Zhou C. Flexible and transparent supercapacitor based on In_2O_3 nanowire/carbon nanotube heterogeneous films. Applied Physics Letters, 2009, 94(4): 043113
67. O'Dwyer C, Szachowicz M, Visimberga G, Lavayen V, Newcomb S B, Torres C M. Bottom-up growth of fully transparent contact layers of indium tin oxide nanowires for light-emitting devices. Nature Nanotechnology, 2009, 4(4): 239–244